

S. Zharikov · R.E. Mennickent · Yu. Shibano · V. Komarova

# Optical spectroscopy of the radio pulsar PSR B0656+14

Received: date / Accepted: date

**Abstract** We have obtained the spectrum of a middle-aged PSR B0656+14 in the 4300-9000Å range with the ESO/VLT/FORS2. Preliminary results show that at 4600-7000Å the spectrum is almost featureless and flat with a spectral index  $\alpha_\nu \simeq -0.2$  that undergoes a change to a positive value at longer wavelengths. Combining with available multiwavelength data suggests two wide, red and blue, flux depressions whose frequency ratio is about 2 and which could be the 1st and 2nd harmonics of electron/positron cyclotron absorption formed at magnetic fields  $\sim 10^8$  G in upper magnetosphere of the pulsar.

**Keywords** Pulsars · Spectroscopy · PSR B0656+14

**PACS** 97.60.Jd

## 1 Introduction

Multiwavelength observations of radio pulsars are an important tool for the study of not yet clearly understood radiative mechanisms and spectral evolution of rotationpowered isolated neutron stars (NSs). Optical observations are an essential part of these studies. Among a dozen optically identified NSs, only seven pulsars have parallax based distances and, therefore, minimal uncertainties ( $\leq 10\%$ ) in luminosities. Their optical spectra are shown in Fig. 1. A reliable optical spectrum has been obtained only for the young and bright Crab pulsar (Sollerman et al. 2000). Other pul-

Based on observations collected at the European Southern Observatory, Paranal, Chile (ESO Programme 074.D-0512A).

S. Zharikov  
OAN IA UNAM, Ensenada, Mexico  
E-mail: zhar@astrosen.unam.mx

R.E. Mennickent  
Universidad de Concepcion, Concepcion, Chile

Yu. Shibano  
Ioffe Physical Technical Inst. RAS, St. Petersburg, Russia

V. Komarova  
Special Astrophysical Observatory, RAS, Russia

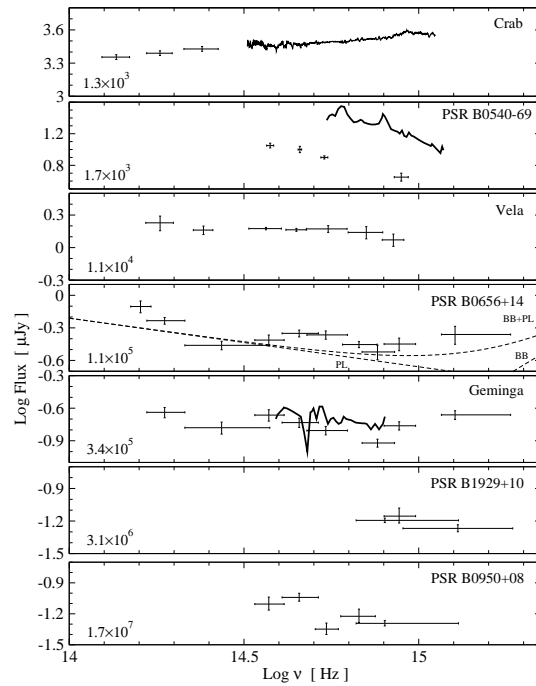


**Fig. 1** Optical spectra of seven pulsars of different characteristic age indicated in the left-bottom corner of each panel in years. The youngest Crab pulsar is at the top and the oldest PSR B0950-08 is at the bottom. For PSR B0656+14 dashed lines show the low energy extensions of the blackbody (BB,  $T=0.84$  MK) and power law (PL,  $\alpha = 0.45$ ) X-ray spectral components and their sum (Koptsevich et al. 2001).

sars are fainter and are represented mainly by broadband photometric points. Published optical spectra of PSR B0540-69 (Hill et al. 1997; Serafimovich et al. 2004) are strongly contaminated by a bright pulsar nebula (Serafimovich et al. 2004), while a tentative spectrum of Geminga (Martin et al. 1998) is much noisier than available photometric fluxes. Mignani et al. (2004) reported on the Vela pulsar spectral observations but these data are not published yet.

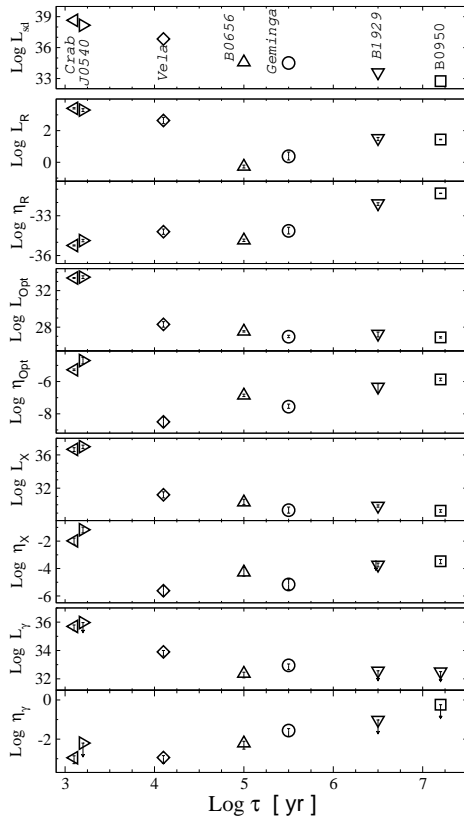


**Fig. 2** From top to bottom: Evolution of the spindown, radio, optical, X-ray, and  $\gamma$ -ray luminosities and respective efficiencies demonstrated by the 7 optical pulsars from Fig. 1.

In Figure 2 we show the evolution of luminosity  $L$  and radiation efficiency  $\eta = L/L_{sd}$  ( $L_{sd}$  is spindown luminosity) demonstrated by these seven pulsars using the data of Table 1 from Zharikov et al. (2006). We note significantly non-monotonic dependencies of  $\eta_{Opt}$  and  $\eta_X$  versus pulsar age with a pronounced minimum at the beginning of the middle-age epoch ( $\simeq 10^4$  yr) and comparably higher efficiencies of younger and older pulsars.

Owing to its relative brightness and proximity, the middle-aged PSR B0656+14 is one of isolated NSs most intensively studied in different wavelengths. It was discovered in radio by Manchester et al. (1978), then identified in X-rays with Einstein, and observed in details with ROSAT, ASCA, Chandra and XMM (for references see Shibano et al. (2005, 2006)). The X-ray emission can be described as a combination of thermal radiation from the entire surface of a cooling NS and from hotter polar caps heated by relativistic particles of magnetospheric origin. An excess over the hot thermal component at energies  $\geq 2$  keV was interpreted as nonthermal radiation from the pulsar magnetosphere (Greiveldinger et al. 1996). The pulsar has been also marginally detected in  $\gamma$ -rays ( $\geq 50$  MeV) by Ramanamurthy et al. (1996).

In the optical PSR B0656+14 was identified by Caraveo et al. (1994) with the ESO/NTT telescopes

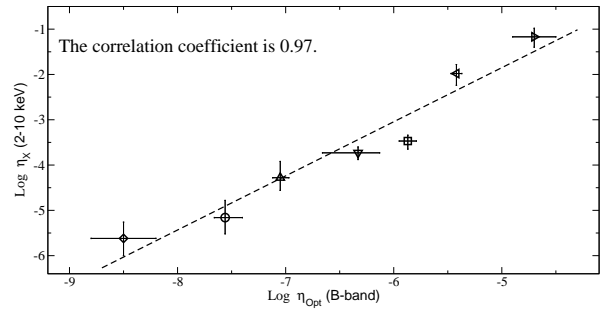


**Fig. 3** Relationship between the B-band optical and 2-10 keV X-ray efficiencies for the same 7 pulsars as in Fig. 1,2.

in the V band. It was then studied in UV with the HST/FOC in the F130LP, F430W, F342W and F195W bands (Pavlov et al. 1997) and with the HST/WFPC in the F555W band (Mignani et al. 1997). Detailed photometric studies in the optical-NIR were performed by Kurt et al. (1998), Koptsevich et al. (2001), Komarova et al. (2003), and Shibano et al. (2006). The studies showed that the bulk of the optical radiation is of nonthermal origin. This was confirmed by the detection of coherent optical pulsations with the radio pulsar period in the B band (Shearer et al. 1997), in a wide 400-600 nm passband (Kern et al. 2003) and in NUV (Shibano et al. 2005). The pulse profiles are rather sharp with a high pulse fraction as expected for nonthermal emission mechanisms. The phase integrated multi-wavelength spectrum (Fig. 4) shows (Koptsevich et al. 2001; Shibano et al. 2006) that the NIR-optical-UV spectral energy distribution is, in a first approach, compatible with the low energy extension of the sum of the X-ray thermal blackbody (BB) spectral component from the whole NS surface and the power law (PL) component dominating in the high energy tail. The BB extension does not contribute at longer wavelengths where the optical-NIR fluxes are in a good agreement with the PL alone (Fig. 1). This indicates a common origin of the nonthermal optical and X-ray emission, which is strongly supported by a good coincidence in phase and shape of the pulse profiles in the optical and the X-ray tail (Shibano et al. 2005). The same origin of the nonthermal optical and X-ray photons is likely to be a general property for other pulsars detected in both ranges, as follows from a strong correlation between respective efficiencies (Fig. 3) found by Zharikov et al. (2004, 2006).

In the optical emission of PSR B0656+14 there is an apparent,  $\simeq(3-5)\sigma$ , flux excess over the PL “continuum” at  $\text{Log}(\nu) \simeq 14.7$  (Fig. 1). This could reveal an additional, 3rd, spectral component to the BB+PL discussed above. Here we present first results of the optical spectroscopy of the pulsar partially motivated by more detailed studies of the excess. In a broader sense, these results also allow us to consider, for the first time, optical properties of a middle-aged ordinary pulsar at the spectroscopic level, as it has been achieved so far only for the Crab pulsar.

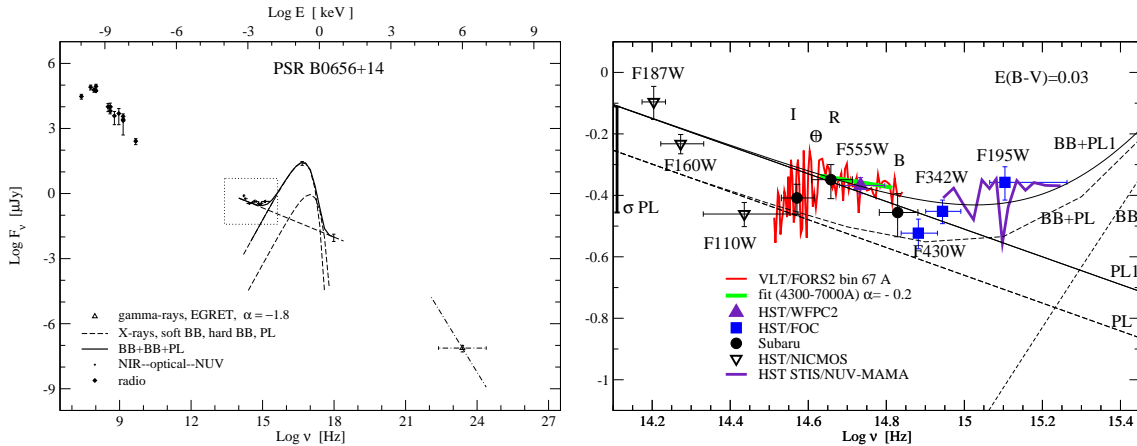


**Fig. 4** *Left*: Unabsorbed multiwavelength spectrum of PSR B0656+14 from the radio through  $\gamma$ -rays. The box marks the range zoomed in the right panel. *Right*: The spectral and photometric fluxes of PSR B0656+14 in the NIR-optical-NUV range obtained with different telescopes and instruments, as notified in the plot. Black dashed lines show low energy extensions of the soft blackbody (BB) and power law (PL) spectral fits and their sum (BB+PL) obtained in X-rays. The black solid lines show the same but with the PL normalization shifted up by a factor of 1.4 (PL1) to fit the upper edge of its  $1\sigma$  error bar shown at the left side of the plot. These are possibly a better match for the optical and NUV spectra than the dashed lines. The symbol  $\oplus$  marks the Earth atmospheric absorption band near  $7600\text{\AA}$ .

## 2 Observations and data analysis

The spectrum of PSR B0656+14 was obtained on November–December 2004 and February 2005 during several observational runs of the ESO program 074.D-0512A using the VLT/UT1 telescope in a service mode. The FORS2<sup>1</sup> instrument was used in a long slit spectroscopic setup with the grating GRIS\_300V and the filter GG435, which cover the wavelength interval of about  $4300\text{--}9600\text{\AA}$  and provide a medium spectral resolution of  $3.35\text{\AA}/\text{pixel}$ . The slit width was  $1''$  and its position angle was selected in a such way as to obtain also spectra of several nearby stars for a sure pulsar astrometric referencing and wavelength/flux calibration. Eighteen 1400 s science spectroscopic exposures were taken with a total exposure time of 25200 s at a mean seeing of  $0.6''$ . Standard reference frames (biases, darks, flatfields, lamps) were obtained in each observational run, while the slit and slitless observations of spectrophotometric standards (Feige110, LTT3218 and LTT1788) for the flux calibration were carried out in separate runs on the same nights.

A combination of the MIDAS and IRAF packages was used for standard CCD data reduction, cosmic-ray track removing, spectra extraction, and subsequent data analysis. A faint,  $R=24.65$ , pulsar is at a limit of spectroscopic capability of the VLT. Nevertheless, excellent seeing conditions allowed us to resolve its spectrum even at each individual exposure, albeit with a low signal to noise ratio S/N. These exposures were co-added. The spectrum was then extracted with a 3 pixel wide extraction slit ( $0.2''/\text{pix}$ ) centered on the pulsar. The backgrounds were extracted with a 6 pixel wide slit centered above and below the center of the pulsar spectrum. The correction

factor for the PSF and sensitivity function were obtained from the Feige110 standard observations. The S/N of the resulting spectrum was about 4 (per pixel) in the  $4450\text{--}5500\text{\AA}$  range and declined to  $\sim 1$  near/above  $8000\text{\AA}$ , due to higher sky backgrounds and a drop in sensitivity towards longer wavelengths. We binned the spectral flux in 20 pixel bins ( $67\text{\AA}$ ) to get S/N near/above 15 and 4, respectively, making the flux accuracy to be comparable with that of available photometric data.

## 3 Results and discussion

The binned and dereddened with  $A_V=0.093$  spectrum of the pulsar is shown in Figure 4 (red curve in the right panel). We show also available multiwavelength data (see Shibanov et al. (2006) for the data and  $A_V$  description). The spectrum is in a good agreement with the broadband VRI fluxes, while it is somewhat higher than the B band flux. It does not show any strong nebular emission lines that could be responsible for the apparent VR excess, mentioned above as a 3rd component, while the presence of weak features can not be completely ruled out. The continuum of the dereddened spectrum in  $4600\text{--}7000\text{\AA}$  range has a power law shape  $\propto \nu^{-0.2\pm 0.2}$  (green line) in agreement with the nonthermal nature of the bulk of the optical emission. Its slope is close to the value expected in this range from the BB+PL extended from X-rays. The slope likely undergoes a change to a positive value between the R and I bands, as follows also from the photometric data.

Within uncertainties the bluest end of the optical and the reddest end of the NUV (Shibanov et al. 2005) spectra are compatible with each other, suggesting a smooth connection of both. However, the F430W photometric

<sup>1</sup> www.eso.org/instruments/fors

flux in the gap between them drops below this connection with a significance of about  $2\sigma$  of the flux confidence level. Unless this is a result of some unknown systematics in calibration, it suggests a spectral dip in the pulsar emission centered near  $\simeq 4300\text{\AA}$  ( $\simeq 14.83$  in  $\text{Log}(\nu)$ ).

The optical and NUV spectra and two NIR photometric points, F160W and F187W, almost perfectly match the BB+PL extension from X-rays, if the PL normalization is taken to be a factor of 1.4 higher (solid lines) than its best X-ray fit value (dashed lines). The change is within  $1\sigma$  uncertainty of the fit. Considering the solid line version as a new optical “continuum level” we find an additional and more significant flux depression in the red part of the spectrum overlapping the I and F110W bands and centered near  $9000\text{-}10000\text{\AA}$  ( $\text{Log}(\nu)\simeq 14.5$ ).

Additional spectral studies are necessary to confirm the suggested “red” and “blue” features and to measure their shapes and wavelengths more accurately. Nevertheless, if they are real, an approximate blue-to-red frequency ratio is  $\simeq 2$ . This indicates that they can be the 1st and 2nd harmonics of an electron/positron cyclotron absorption formed in the upper magnetosphere of the pulsar at an effective altitude where the magnetic field  $B\simeq 10^8$  G. This is  $\simeq 360$  km, assuming a dipole NS field with a surface value of  $4.66\times 10^{12}$  G, as derived from spindown measurements. The absorbing  $e^\pm$  have to be cooled enough and provide a sufficient optical depth above a source of the nonthermal continuum. The source altitude is, therefore,  $<360$  km and much below the light cylinder radius of  $\simeq 18\times 10^3$  km, likely suggesting its polar cap origin. The features are broad, as expected from the magnetospheric field inhomogeneity. Tentative ( $\leq 2\sigma$ ) absorption features in the NUV spectrum at  $\text{Log}(\nu)\simeq 15$  and 15.1 (Shibanov et al. 2005) may be the 3rd and 4th harmonics, respectively, which are fainter as the cyclotron harmonic intensity decreases with its number  $n$ .

Similar, albeit less significant, spectral features are likely seen in the photometric and spectral data of another middle-aged pulsar Geminga (Fig.1). The absence of strong nebular lines suggests that the features are also of the NS magnetospheric origin. To explain the Geminga spectrum Martin et al. (1998) applied a toy model of an ion cyclotron absorption at  $B\simeq 10^{11}$  G in the inner magnetosphere of the NS combined with the BB and PL components. At this field a low  $n$  ion cyclotron frequencies indeed fall in the optical range. However, it is likely that the nonthermal optical emission is generated in the upper magnetosphere where the magnetic field is by orders of magnitude weaker and any ion cyclotron absorption of the respective optical continuum is negligible. In this case the electron/positron cyclotron absorption or scattering appears to be more plausible interpretation.

The optical spectrum of the young Crab-pulsar is featureless and has a different (positive) slope (Fig. 1). The ten times older Vela-pulsar has a flat and also featureless spectrum (Mignani, private communication). The spec-

trosopy of PSR B0656+14 demonstrates that optical spectra of middle-aged pulsars can be distinct from those of younger ones by the presence of unusual spectral features or slope changes. To study this new spectral observations of PSR B0656+14 in the NIR and  $3000\text{-}5000\text{\AA}$  ranges are needed. A question, whether the observed difference in pulsar spectra is simply caused by different pulsar geometry or by a change of physical conditions in the emission region with age, demands quantitative modeling physical processes in pulsar magnetospheres.

**Acknowledgements** The work was partially supported by DGAPA/PAPIIT project IN101506, CONACYT 48493, RFBR (grants 05-02-16245, 05-02-22003) and Nsh 9879.2006.2. REM was supported by Fondecyt 1030707.

## References

- Caraveo, P., Bignami, G. F., Mereghetti, S. *ApJL* **422**, 82 (1994)
- Greiveldinger, C., Camerini, U., Fry, W. et al. *ApJL* **465**, 35 (1996)
- Hill, R. J., Dolan, J. F., Bless, R. C., et al. *ApJL* **486**, 99 (1997)
- Manchester, R. N., Lyne, A. G., Taylor, J. H., et al. *MNRAS* **185**, 409 (1978)
- Martin, C., Halpern, J., Schiminovich, D. *ApJL* **494**, 211 (1998)
- Mignani, R., Caraveo, P. A., Bignami, G. F. *The Messenger* **87**, 43 (1997)
- Mignani, R. P., de Luca, A., Caraveo, P. A. :In: F. Camilo and B. M. Gaensler (ed) *Proceedings of the IAU Symposium no. 218 “Young Neutron Stars and Their Environments”*, held as part of the IAU General Assembly, 14-17 July, 2003 in Sydney, Australia. *Astronomical Society of the Pacific*, 391 (2004)
- Kern, B., Martin, C., Mazin, B., Halpern, J. P. *ApJ* **597**, 1049 (2003)
- Koptsevich, A. B., Pavlov, G. G., Zharikov, S. V., et al. *A&A* **370**, 1004 (2001)
- Komarova, V., Shibanov, Yu., Zharikov, S., et al. In: G. Cusumano, G., Massaro, E., Mineo, T. (ed.) *Proceedings of the International Workshop Pulsars, AXPs and SGRs observed with BeppoSAX and Other Observatories held in Marsala, Italy, September 23-25, 2002*. 77 *Aracne Editrice*, (2003)
- Kurt, V. G., Sokolov, V. V., Zharikov, S. V. et al. *A&A* **333**, 547 (1998)
- Pavlov, G. G., Welty, A. D., Cordova, F. A. *ApJ* **489**, L75 (1996)
- Ramanamurthy, P., Fichtel, C., Harding, A., et al. *A&ASS* **120**, 115 (1996)
- Serafimovich, N. I., Shibanov, Yu. A., Lundqvist, P., Sollerman, J., *A&A* **425**, 1041
- Shearer, A., Redfern, R. M., Gorman, G., et al. *ApJL* **487**, 181 (1997)
- Shibanov, Yu. A., Sollerman, J., Lundqvist, P., et al. *A&A* **440**, 693 (2005)
- Shibanov, Y. A., Zharikov, S. V., Komarova, V. N, et al. *A&A* **448**, 313 (2006)
- Sollerman, J., Lundqvist, P., Lindler, D., et al. *ApJ* **537** 861 (2000)
- Zharikov, S. V., Shibanov, Yu. A., Mennickent, R. E., et al. *A&A* **417**, 1017 (2004)
- Zharikov, S., Shibanov, Yu., Komarova, V. *AdSpR* **37**, 1979 (2006)